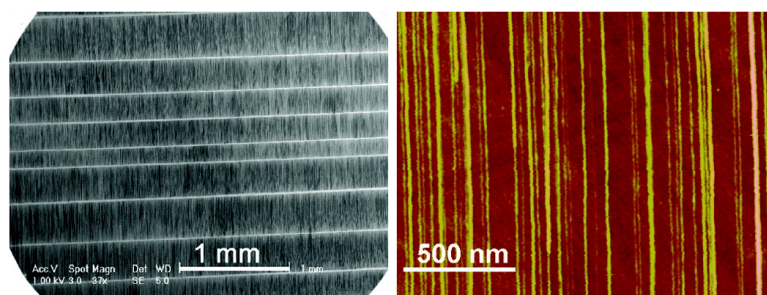


## Growth of High-Density Parallel Arrays of Long Single-Walled Carbon Nanotubes on Quartz Substrates

Lei Ding, Dongning Yuan, and Jie Liu

*J. Am. Chem. Soc.*, **2008**, 130 (16), 5428-5429 • DOI: 10.1021/ja8006947 • Publication Date (Web): 01 April 2008

Downloaded from <http://pubs.acs.org> on February 8, 2009



### More About This Article

Additional resources and features associated with this article are available within the HTML version:

- Supporting Information
- Links to the 7 articles that cite this article, as of the time of this article download
- Access to high resolution figures
- Links to articles and content related to this article
- Copyright permission to reproduce figures and/or text from this article

[View the Full Text HTML](#)

## Growth of High-Density Parallel Arrays of Long Single-Walled Carbon Nanotubes on Quartz Substrates

Lei Ding, Dongning Yuan, and Jie Liu\*

Department of Chemistry, Duke University, Durham, North Carolina 27708

Received January 28, 2008; E-mail: j.liu@duke.edu

The unique properties of single-walled carbon nanotubes (SWNTs) and their potential applications in logic circuits, field effect transistors, and sensors make SWNTs important materials in nanoscience and nanotechnology.<sup>1–4</sup> To fully utilize the outstanding electronic properties of the nanotubes, the growth of horizontally well-aligned carbon nanotube arrays on suitable substrates is a critical step for large scale, low-cost fabrication of nanotube electronic devices. Compared with random networks of SWNTs on surface, the aligned SWNTs can avoid the overlap of the nanotubes and the resistance caused by the nanotube junctions. Until now, aligned SWNTs have been obtained through a self-assembly<sup>5</sup> method and direct growth approaches with the assistance of electric field<sup>6</sup> and feeding gas flow.<sup>7,8</sup> However, it remains difficult to produce aligned SWNTs arrays over large areas with high density, which would limit the use of SWNTs in realistic devices for their low current outputs and small active areas. Now, surface lattice guided growth of SWNTs by chemical vapor deposition (CVD) has been an important advance for its high density and well alignment. Using this method, researchers can obtain well-aligned arrays of SWNTs on single crystal surfaces including sapphire<sup>9–12</sup> and quartz.<sup>13,14</sup> Recently, Rogers' group used quartz wafers preannealed at 900 °C for 8 h as substrates for the growth of perfectly aligned arrays of SWNTs with density as high as 10 SWNTs/ $\mu\text{m}$ .<sup>15,16</sup> In these recent works, iron catalysts including ferritin and evaporated iron film were always used as the catalyst. Several growth mechanisms such as "wake up",<sup>9</sup> "raised head",<sup>12</sup> and "top-growth"<sup>17</sup> mechanisms have been presented. However, direct proofs are lacking. Additionally, the alignment of the nanotubes is thought to be caused by surface steps formed by long-time thermal annealing. Herein we report a CVD approach to prepare high-density and perfectly aligned arrays of long SWNTs on stable temperature (ST)-cut quartz substrates using copper as the catalyst and ethanol as the carbon source. Compared with earlier reports, we have demonstrated that the aligned nanotube arrays can be grown on ST quartz substrate without the need of thermal annealing. The density can reach >50 nanotubes per micron and the length can be a few millimeters (Figure 1 and Supporting Information). Such high density aligned nanotube films can find immediate applications in high current and high frequency devices. Additionally, we have obtained direct proof on the "tip-growth" mechanism for the aligned nanotubes and important evidence that explained the termination of the growth.

The substrates used in the CVD approach were single-crystal ST-cut quartz wafer obtained from Hoffman Materials Inc. without any further treatment. The  $\text{CuCl}_2$ /polyvinylpyrrolidone (PVP) alcohol solution, used as the catalyst solution, was patterned onto the quartz surface by two ways. The first was achieved by the spin-coating method with 4000 rpm. The second

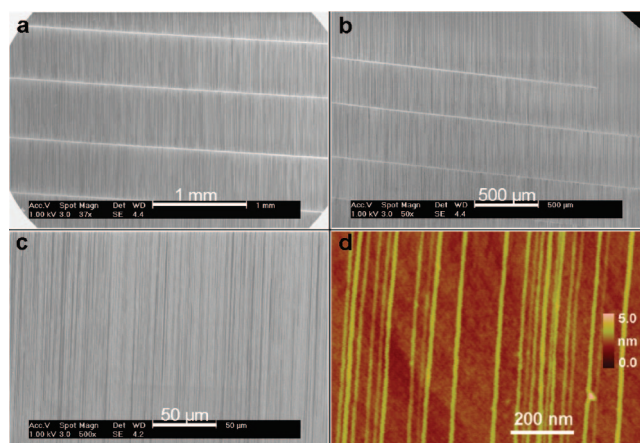


**Figure 1.** SEM and AFM images of high-density and perfectly aligned arrays of long SWNTs along [100] direction on the ST-cut quartz substrate using patterned copper catalyst. The bright stripes in (a) and (b) correspond to copper catalyst. (c) High-magnification SEM image of the arrays of SWNTs. (d) AFM image of  $1 \mu\text{m} \times 0.75 \mu\text{m}$  area, in which 22 SWNTs have been found.

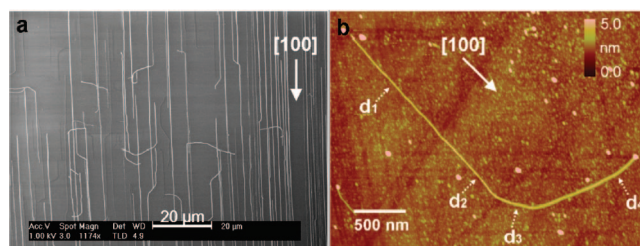


**Figure 2.** SEM and AFM images of SWNTs grown on ST-cut quartz using spin cast  $\text{CuCl}_2$ /PVP as the catalyst. The [100] crystallographic direction was marked with the arrow.  $d_1$ – $d_4$  represent the diameter values of the SWNT at different positions marked with dotted arrows.

was achieved with a mask method. Briefly, a mask with line patterns on it was glued onto the quartz surface. Then the catalyst solution was dropped onto the mask and evaporated. Lastly, the mask was removed from the quartz surface to leave the line-shape patterns of catalyst generated on the substrate. The substrate was then treated with oxygen plasma for 15 min, followed by CVD growth of SWNTs at 900 °C with a flow of hydrogen (400 sccm) and argon (150 sccm, through an ethanol bubbler). After 15 min of growth, the sample was cooled to room temperature and inspected with scanning electron microscopy (SEM), atomic force microscopy (AFM), and RAMAN spectrometer.

Figure 2a shows an SEM image of SWNTs grown on ST-cut quartz with spin cast  $\text{CuCl}_2$ /PVP as catalyst where the catalyst nanoparticles are uniformly distributed over the substrate. From

the SEM image, it is obvious that nanotubes form a parallel array and the length is a few tens to hundreds of microns. The orientations of SWNTs are found to align along the X direction of the ST-cut single crystal quartz, which is equivalent to the [100] crystallographic direction, regardless of the gas flow direction. Another interesting observation is that some of the nanotubes bent to form a “sickle” shaped structure. To understand the formation of such “sickle” structures, AFM was used to inspect these SWNTs carefully. Figure 2b displays an AFM image of one such SWNT, part of which is aligned to the X direction while the other part is curved. From the figure, three important observations can be found: First, the SWNT has uniform diameter at the straight part with values  $d \approx d_1 \approx d_2 \approx 1.6$  nm. But the diameter of the curved part of the SWNT becomes larger. The diameter of the SWNT was found to change from 1.6 to 1.9 nm ( $d_3$ ) and 2.1 nm ( $d_4$ ). Second, the catalyst nanoparticle was found at the top of the curved part with a diameter of 7.1 nm. Third, no atomic steps were observed in the image, unlike results from earlier reports on the growth of aligned nanotubes on quartz substrates.<sup>13</sup> These observations can be explained with a hypothesis of a “tip-growth” mechanism where the catalyst nanoparticles slide on the substrate. The growth process of the “sickle” SWNTs can be divided into two steps. First, the SWNT grows along the X direction on the surface with catalyst on the tip and sliding along the X direction of the substrate. The diameter of the catalyst is relative small. Second, as the nanotubes grow longer, the catalyst nanoparticles collide with other metal nanoparticles on the surface. The catalyst nanoparticles merge together to form bigger particles. As a result of the increase in the sizes of catalyst nanoparticles, the diameter of the SWNTs increases. As the diameters of the catalyst nanoparticles become too big to have strong anisotropic interaction with the surface lattice of the substrate, the alignment of the nanotubes to the surface lattice become not energetically preferred and the nanotubes start bending, leading to the formation of “sickle” SWNTs. Finally, the nanotubes stop growing either by running into another nanotube on the surface or because the increase in the size of nanoparticles makes the catalyst not active for continued growth of nanotubes. In other words, the changing of the diameter of the catalyst nanoparticles caused by the collision with other catalyst nanoparticles is responsible for the bending and growth termination of the nanotubes. More proofs for the tip-growth mechanism are shown in the Supporting Information.

To avoid such influence of unreacted catalyst nanoparticles on the surface, we used patterned copper catalyst for the growth of SWNTs on ST-cut quartz. Figure 1 presents the SEM and AFM images of results. The high-density and perfectly aligned arrays of long SWNTs have been found on the whole ST-cut quartz substrate. The distance between the catalyst lines was 600  $\mu\text{m}$  in Figure 1a and 400  $\mu\text{m}$  in Figure 1b. Most of the SWNTs can grow as long as the distance between the patterned lines. Figure 1c is the high-magnification SEM image of the perfectly aligned arrays of SWNTs along with X direction. No curved or random SWNTs have been found in the image. Figure 1d presents an AFM image of 1  $\mu\text{m}$   $\times$  0.75  $\mu\text{m}$  area, in which 22 SWNTs have been found. As can be observed from the image, the change in the nanotube diameter is not present, unlike the nanotubes growth from spin cast catalysts. The explanation for such differences is that these nanotubes grown from patterned catalysts do not run into other catalysts during growth and thus the diameters of the nanotubes do not change and the lengths can be much longer until they run into another catalyst pattern on the surface. As shown in the Supporting Information,

nanotubes up to a millimeter long can be grown easily and the highest density of nanotubes can reach >50 nanotubes per micron to the degree that they are not distinguishable from each other under AFM due to the limited resolution of the instrument (Supporting Information). To the best of our knowledge, it is the highest density of aligned SWNTs reported. The histogram of the SWNTs diameter distribution reveals a narrow distribution of  $1.2 \pm 0.3$  nm (Supporting Information). Also, the radical breathing mode (RBM) signal at 189  $\text{cm}^{-1}$  and G-band at 1593  $\text{cm}^{-1}$  were clearly observed (Supporting Information).

In summary, we discovered a method to grow high-density, uniform, perfectly aligned arrays of long SWNTs on ST-cut quartz using copper as the catalyst and ethanol as the carbon source. We have also observed the formation of “sickle” shaped nanotubes when using spin cast nanoparticles as catalysts. The increase in the sizes of the catalyst nanoparticles as a result of merging with unreacted nanoparticles on the substrate surface is believed to be the cause of bending and termination of nanotubes. With the understanding of the impacts caused by nanoparticles merging, a patterned catalyst is used to avoid the effect for the growth of long and straight nanotubes with high density. The length of the nanotubes can be controlled by the spacing between catalyst patterns, and the diameter has an intrinsically narrow distribution around 1.2 nm. Such high-density perfectly aligned nanotubes can be directly used for high current and high frequency electronic devices. The uniformity and the alignment make the fabrication of nanotube devices more straightforward. We believe that our method for the growth of high-density aligned SWNTs will find wide applications for practical nanotube devices.

**Acknowledgment.** The work was supported in part by a grant from NRL (N00173-04-1-G902) and a fund from Duke University. L.D. thanks Professor Yan Li at Peking University and Dr. Weiwei Zhou at UC Irvine for helpful discussions.

**Supporting Information Available:** SEM and AFM images of long and high density arrays of carbon nanotubes and their RAMAN Spectra as well as diameter distribution. This material is available free of charge via the Internet at <http://pubs.acs.org>.

## References

- (1) Dresselhaus, M. S.; Dresselhaus, G.; Avouris, P. *Carbon Nanotubes: Synthesis, Structure, Properties and Applications*; Springer-Verlag: Berlin, 2001.
- (2) Bachtold, A.; Hadley, P.; Nakanishi, T.; Dekker, C. *Science* **2001**, *294*, 1317.
- (3) Tans, S.; Verschueren, A.; Dekker, C. *Nature* **1997**, *386*, 474.
- (4) Kong, J.; Franklin, N.; Zhou, C.; Pan, S.; Cho, K.; Dai, H. *Science* **2000**, *287*, 622.
- (5) Rao, S. G.; Huang, L.; Setyawan, W.; Hong, S. *Nature (London)* **2003**, *425*, 36.
- (6) Ural, A.; Li, Y.; Dai, H. *Appl. Phys. Lett.* **2002**, *81*, 3464.
- (7) Huang, S.; Maynor, B.; Cai, X.; Liu, J. *Adv. Mater.* **2003**, *15*, 1651.
- (8) Zhou, W.; Han, Z.; Wang, J.; Zhang, Y.; Jin, Z.; Sun, X.; Zhang, Y.; Yan, C.; Li, Y. *Nano Lett.* **2006**, *6*, 2987.
- (9) Ismach, A.; Segev, L.; Wachtel, E.; Joselevich, E. *Angew. Chem., Int. Ed.* **2004**, *43*, 6140.
- (10) (a) Han, S.; Liu, X.; Zhou, C. *J. Am. Chem. Soc.* **2005**, *127*, 5294. (b) Ismach, A.; Kantorovich, D.; Joselevich, E. *J. Am. Chem. Soc.* **2005**, *127*, 11554.
- (11) Ago, H.; Nakamura, K.; Ikeda, K.; Uehara, N.; Ishigami, N.; Tsuji, M. *Chem. Phys. Lett.* **2005**, *408*, 433.
- (12) Yu, Q.; Qin, G.; Li, H.; Xia, Z.; Nian, Y.; Pei, S.-S. *J. Phys. Chem. B* **2006**, *110*, 22676.
- (13) Kocabas, C.; Hur, S. H.; Gaur, A.; Meitl, M. A.; Shim, M.; Rogers, J. A. *Small* **2005**, *1*, 1110.
- (14) Kocabas, C.; Shim, M.; Rogers, J. A. *J. Am. Chem. Soc.* **2006**, *128*, 4540.
- (15) Kang, S. J.; Kocabas, C.; Ozel, T.; Shim, M.; Pimparkar, N.; Alam, M. A.; Rotkin, S. V.; Rogers, J. A. *Nat. Nanotechnol.* **2007**, *2*, 230.
- (16) Kang, S. J.; Kocabas, C.; Kim, H.-S.; Cao, Q.; Meitl, M. A.; Khang, D.-Y.; Rogers, J. A. *Nano Lett.* **2007**, *7*, 3343.
- (17) Su, M.; Li, Y.; Maynor, B.; Buldum, A.; Lu, J. P.; Liu, J. *J. Phys. Chem. B* **2000**, *104*, 6505.

JA8006947